9

N-Shots 2*N*-Phase-Steps Binary Grating Interferometry

Cruz Meneses-Fabian, Gustavo Rodriguez-Zurita
and Noel-Ivan Toto-Arellano
Facultad de Ciencias Físico-Matemáticas,
Benemérita Universidad Autónoma de Puebla
México

1. Introduction

In physical optics, the interference effect consists in superposing two or more optical fields in a region of space, which mathematically results in the vector sum of them, it is certain because of in physical optics the superposition principle is valid. So, when this sum is observed with some optical detector such as a human eye or a CCD camera, the irradiance of the total field is obtained, and it can be understood as the sum of the irradiance from each individual field, known as background light, plus an interference additional term per each pair of fields, which consists of a cosine of the phase difference between the two waves and of a factor given mainly by the product of waves amplitudes known as a modulation light. The total effect shows brilliant and obscure zones known as interference fringes, also called as a fringe pattern, or an interferogram (Born & Wolf, 1993). This effect was first reported by Thomas Young in 1801 (Young, 1804; Shamos, 1959), more late it also was observed by Newton, Fizeau, Michelson, etc. (Hecht, 2002). They designed many optical arranges now known as interferometers in order to interfere two o more waves trying to meet the optimal conditions to have a maximum quality in the fringes. Many studies have demonstrated that the fringe quality, (better known as visibility of interference pattern), as well as the shape and the number of fringes is depending of each parameter in the optical field such as the amplitude, the polarization state, the wavelength, the frequency, the coherence degree, the phase and because of it so many applications among physics and other sciences like biology, medicine, astronomy, etc., or also in engineering have been extensively made (Kreis, 2005). However, an intermediate step between the fringe pattern and the direct application in some topic of interest as the evaluation and processing of this pattern must be realized. In this regarding, many proposal have been amply discussed, for example in interferometry of two waves when the phase difference is the variable to be calculated, one of the techniques more widely used consists of performing consecutively shifts of constant phase between the waves that interfere. Then, for each phase-step a new interferogram is gotten and therefore for N steps, N interferograms are obtained. Mathematically, a Nx3 system of equations is formed since the with phase-step the object phase, the background light, and the modulation of light are considered unknown with respect to position and constant with respect to time, is known as phase-shifting interferometry (PSI) (Creath, 1993; Malacara, 2007; Schwider, 1990). The phase shift is introduced by a shifting device, which can be done

with Zeeman effect shifters, acousto-optical modulators, rotating polarizers or translating gratings, among other possibilities. Spatial techniques also have been introduced and widely studied. These consist of introducing a spatial phase variation into interferogram (Takeda, et. al., 1982). Typically, this variation is a linear function, but when the fringes forms closed loops this carrier is not appropriate, and to overcome this shortage a quadratic phase has been proposal (Malacara, et. al., 1998). Others methods for phase extraction have also been proposed (Moore & Mendoza-Santoyo, 1995; Peng, et. al., 1995).

Based on the interference of two monochromatic and coherent waves, the present chapter speaks about the phase shifting interferometry. The principal idea consists of obtaining two interferograms shifted in phase by 180° in a single-shot. By performing an arbitrary phase-step, another two interferograms shifted 180° in phase are captured in a second shot. This way, four interferograms result shifted in phase in two shots with two phase steps, considering the first phase step equal to zero. The arbitrary phase-step is considered to be between 0° and 180° and it will be measured under the concept of generalized phase-shifting interferometry (GPSI) (Xu, et. al., 2008). Therefore, in general with N-phase-steps $2N$ interferograms will be captured in N shots only. Fringe patterns are obtained from an interferometer build using a $4f$ optical correlator of double Fourier transform, where, at the input plane two apertures are considered. One of them is crossed by a reference beam and the other is considered as a probe window where a phase object is placed. These windows are considered as an input transmittance function. In the Fourier plane, a binary grating (Ronchi ruling) with certain period is placed as a spatial filter function. Then with the appropriate conditions of the wavelength, the grating period, and the focal length of the lenses, at the image plane the interference of the fields in each window is achieved and replicated around diffraction order. Then, by using orthogonal linear polarization in the windows, it is possible to demonstrate that a phase shifting of 180° can be obtained by observing the superposition with adequate transmittance angle of another linear polarizer. An arbitrary phase-shifting is later obtained with a grating displacement.

In summary, a method to reduce the number of captures needed in phase-shifting interferometry is proposed on the basis of grating interferometry and modulation of linear polarization. In this chapter, the case of four interferograms is considered. A common-path interferometer is used with two windows in the object plane and a Ronchi grating as the pupil, thus forming several replicated images of each window over the image plane. The replicated images, under proper matching conditions, superimpose in such a way so that they produce interference patterns. Orders 0 and +1 and -1 and 0 form useful patterns to extract the optical phase differences associated to the windows. A phase of π is introduced between these orders using linear polarizing filters placed in the windows and also in the replicated windows, so two π-shifted patterns can be captured in one shot. An unknown translation is then applied to the grating in order to produce another shift in the each pattern. A second and final shot captures these last patterns. The actual grating displacement and the phase shift can be determined according to the method proposed by (Kreis, 1986) before applying proper phase-shifting techniques to finally calculate the phase difference distribution between windows. Along this chapter a theoretical model is amply discussed and it is verified with both a numeral simulation and experimental results.

2. Theoretical analysis

Phase-shifting interferometry retrieves phase distributions from a certain number N of interferograms (Creath, 1993; Malacara, 2007). Each interferogram I_k must result from

phase displacements by certain phase amounts φ_k $(k=0\ldots N-1)$ in order to form a solvable system of equations (Malacara, et. al., 1998; Creath, 1993; Millerd & Brock, 2003). Because one of these phase amounts can be taken as reference, say $\varphi_0=0$, it is possible to use the corresponding phase shifts, each denoted by $\alpha_{k+1}=\varphi_{k+1}-\varphi_k$. Among several possibilities, the case of $N=4$ interferograms and $N-1=3$ equal shifts $\alpha_1=\alpha_2=\alpha_3=\alpha=90°$, has been demonstrated to be very useful (Schreiber & Bruning, 2007;), especially for well contrasted interferograms (Schwider, 1990). To obtain phase-shifted interferograms, a number of procedures have been demonstrated but many of them needs of *N* shots to capture all of those interferograms. Thus, a simplification is desirable in order to reduce the time of capture. Single-shot interferometers capturing all needed interferograms simultaneously are good examples of this effort (Barrientos-Garcia, et. al., 1999; Novak, 2005). On the other side, phase shifts can be induced by mechanical shifts of a proper element, as a piezoelectric stack (Bruning, et. al., 1974) or a grating (Schwider, 1990). Modulation of polarization is another useful technique (Creath, 1993). In grating interferometry, a grating can be transversally displaced by a quarter of a period to obtain shifts of $\alpha=90°$ (Meneses-Fabian, et. al., 2006), for example. But in order to obtain several values, the same number of displacements is required (Hariharan, et. al., 1987; Hu, et. al., 2008; Novák, et. al., 2008). Besides, when using gratings as phase shifters, the grating displacement must be carried out with sufficient precision. The higher the grating frequency, the smaller the grating displacement required. Thus, the use of high frequency rulings could compromise the precision of the phase shift.

In this chapter, a method to reduce the number of captures from 2*N* to *N* is proposed by means of common-path grating interferometry (Meneses-Fabian, et. al., 2006) in conjunction with crossed linear polarization filters for modulation of polarization (Nomura, et. al., 2006) and grating displacements. A common-path phase-shifting interferometer can be constructed with two-window in the object plane of a 4*f* Fourier-transform system and a grating as its pupil (Arrizon & De-La-Llave, 2004). One-shot phase-shifting interferometers have already been proposed with phase-gratings and elliptical polarization (Rodriguez-Zurita, et. al., 2008a; Kreis, 1986). However, a more common Ronchi grating can be used for the case of $N=4$ because the diffraction efficiencies for diffraction orders ±1 are sufficiently good enough to display adequate interferograms. Interference of first-neighboring orders can be obtained in the image plane when proper matching conditions are fulfilled and the phase shifting can be performed with grating displacement driven by an actuator (Meneses-Fabian, et. al., 2006). Because several diffraction orders are to be found in the image plane, some additional shifts can be induced by use of linear polarization instead of circular or elliptical polarization. The calculation of the values of the shifts induced by a grating displacement can be carried out with a method developed by Thomas Kreis (Kreis, 1986), thus alleviating the need of a more detailed calibration. This method is particularly useful for the case of $N=4$, where the proposed simplification reduces the number of required grating displacements to only one. This particular value does not need to be known beforehand because it can be calculated directly by the above mentioned method of Kreis to find a solution for the optical phase. Then, the number of shots required to capture the four interferograms would result in only two. We restricted ourselves to the case of $N=4$ precisely but with α_i not necessarily of the same value. Experimental results are presented.

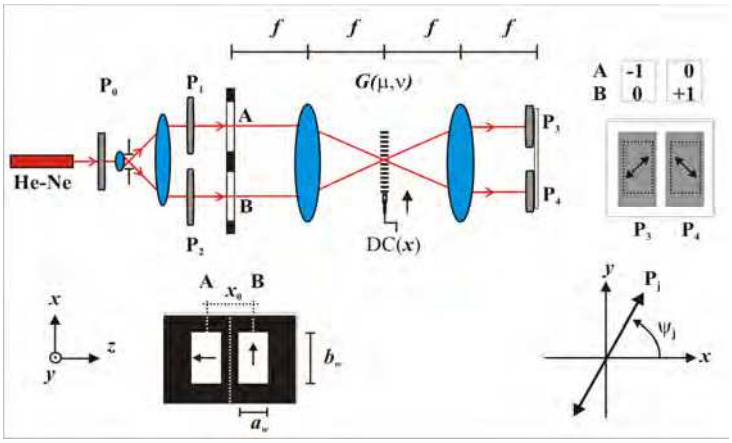

Fig. 1. Experimental setup. Pj , j = 0…4: linear polarizers. A, B: rectangular windows in object plane. $G(\mu,\nu)$: Ronchi grating (μ,ν the spatial frequencies escalated by λf). DC(x): actuator. f: focal length. Side views of windows (lower left) and polarizers with $\psi = \psi_j$ in image plane (lower right) are also sketched.

2.1 Theoretical background

Fig.1 shows the experimental setup. It comprises a 4*f* Fourier-transform system under monochromatic illumination at wavelength λ. The transforming lenses have a focal length of *f*. Linear polarizer P_0 have its transmission axis at 45° and the linear polarizers P_1 and P_2, over windows A and B, have its transmission axis at 0° and 90° respectively. The object plane (input plane) consists of two similar rectangular windows A and B, each of sides a_w and b_w. The windows centers are separated by the distance x_0. In general, an amplitude distribution of the form $A(x,y)$ can be considered in the window A as a reference wave, while $B(x,y)\exp\left[i\phi(x,y)\right]$ can represent the amplitude distribution in the window B (a test object, for instance). Then, the input transmittance can be expressed by.

$$\mathbf{t}(x,y) = w(x+\frac{1}{2}x_0,y)A\left(x+\frac{1}{2}x_0,y\right)\mathbf{J}_A + w(x-\frac{1}{2}x_0,y)B\left(x-\frac{1}{2}x_0,y\right)\exp\left[i\phi\left(x-\frac{1}{2}x_0,y\right)\right]\mathbf{J}_B \quad (1)$$

where $\mathbf{J}_A = \begin{pmatrix}1\\0\end{pmatrix}$, $\mathbf{J}_B = \begin{pmatrix}0\\1\end{pmatrix}$ are Jones vectors corresponding to orthogonal linear polarization states and the window function is written as $w(x,y) = rect\left(x/a_w\right)\cdot rect\left(y/b_w\right)$, where $rect\left(x/a_w\right)$ is the rectangle function on x direction of width a_w and $rect\left(y/b_w\right)$ is the rectangle function on y direction of width b_w.

A binary absorptive grating $G(\mu,\nu)$ with spatial period u_d and bright-band width u_w is placed in the frequency plane (Fourier plane, Fig.1). An actuator (DC) can translate the grating longitudinally through a given distance u_0. The grating (a Ronchi grating) can be written.

$$G(\mu,\nu)=rect\left(\frac{\mu-\mu_0}{\mu_w}\right)\otimes\sum_{n=-\infty}^{\infty}\delta(\mu-n\mu_d)\,, \tag{2}$$

with the spatial frequency coordinates are given by $(\mu,\nu)=(u/\lambda f, v/\lambda f)$, where (u,v) are the actual spatial coordinates, and $\mu_k=u_k/\lambda f$ with $k=0,w,d$ as a label for displacement, bright-band width and grating period, respectively. The symbol $\otimes$ means convolution.

In the image plane, the amplitude distribution can be written as the convolution between the amplitude of the object and the impulse response of the system, i.e.,

$$\mathbf{t}_O(x,y)=\mathbf{t}(x,y)\otimes\Im^{-1}\{G(\mu,\nu)\}\,, \tag{3}$$

with $\Im^{-1}$ the inverse Fourier-transform operation assumed to be performed by the second transforming lens as a convention taken in this work in accordance with an inversion in the image coordinates. Using Eq. (2), the convolution results in

$$\mathbf{t}_O(x,y)=\sum_{n=-\infty}^{\infty}C_n\left\{w_A\left[x-\left(\frac{n}{N_0}-\frac{1}{2}\right)x_0,y\right]\mathbf{J}_A+w_B\left[x-\left(\frac{n}{N_0}+\frac{1}{2}\right)x_0,y\right]\exp\left[i\phi\left(x-\left(\frac{n}{N_0}+\frac{1}{2}\right)x_0,y\right)\right]\mathbf{J}_B\right\}, \tag{4}$$

where $w_A(x,y)=w(x,y)A(x,y)$ and $w_B(x,y)=w(x,y)B(x,y)$ have been defined and $\Im^{-1}\{G(\mu,\nu)\}=\sum_{n=-\infty}^{\infty}C_n\delta(x-n/\mu_d)$ has been substituted with $C_n=\frac{1}{2}\mathrm{sinc}(n/2)\exp(i2\pi n u_0/u_d)$ for $\mu_w=\frac{1}{2}\mu_d$, and assuming that x_0 equals some multiple integer N_0 of the period, in other words, $x_0=N_0/\mu_d=N_0(\lambda f/u_d)$, (diffraction orders matching condition). According to Eq. (4), the amplitude in the image plane consists of a row of copies of the entrance transmittance, each copy separated by $1/\mu_d=\lambda f/u_d$ from the first neighbours. By adjusting the distance x_0 between windows such that $N_0/\mu_d=x_0$ and also assuring that the inequality $a_w\le\lambda f/u_d$ is satisfied, the field amplitude $\mathbf{t}_w(x,y)$ of window $w[x-(n/N_0-1/2)x_0,y]$ (as observed through a linear polarizer with transmission axis at angle ψ_n with respect to the horizontal) can be described as

$$\mathbf{t}_w(x,y)=\left\{C_nA(x,y)\cos(\psi_n)+C_{n-N_0}B(x,y)\sin(\psi_n)\exp[i\phi(x,y)]\right\}\mathbf{J}_\psi\,. \tag{5}$$

where $\cos(\psi_n)\mathbf{J}_\psi=\mathbf{J}_\psi^L\mathbf{J}_A$, $\sin(\psi_n)\mathbf{J}_\psi=\mathbf{J}_\psi^L\mathbf{J}_B$, and

$$\mathbf{J}_\psi^L=\begin{pmatrix}\cos^2(\psi_n) & \sin(\psi_n)\cos(\psi_n)\\ \sin(\psi_n)\cos(\psi_n) & \sin^2(\psi_n)\end{pmatrix};\qquad \mathbf{J}_\psi=\begin{pmatrix}\cos(\psi_n)\\ \sin(\psi_n)\end{pmatrix}. \tag{6}$$

In particular, for the case $N_0=1$ and knowing that the irradiance results proportional to the square modulus of the field amplitude, $I(x,y)=|\mathbf{t}_w(x,y)|^2$, the corresponding interference pattern is given by

$$I(x,y)=a_n(x,y)+b_n(x,y)\cos\left[\phi(x,y)-2\pi\frac{u_0}{u_d}\right], \tag{7}$$

where $a_n(x,y)$ is known as background light, $b_n(x,y)$ is known as a modulation light and they are given by

$$a_n(x,y)=\frac{1}{4}\mathrm{sinc}^2\left(\frac{1}{2}n\right)\cos^2\psi_n I_A(x,y)+\frac{1}{4}\mathrm{sinc}^2\left(\frac{1}{2}(n-1)\right)\sin^2\psi_n I_B(x,y), \tag{8a}$$

$$b_n(x,y)=\frac{1}{4}\mathrm{sinc}\left(\frac{1}{2}n\right)\mathrm{sinc}\left[\frac{1}{2}(n-1)\right]\sin(2\psi_n)\sqrt{I_A(x,y)I_B(x,y)}, \tag{8b}$$

with $I_A(x,y)=|A(x,y)|^2$ and $I_B(x,y)=|B(x,y)|^2$. The pattern in Eq. (7) results to be modulated by the functions sin and sinc. Note that $a_n(x,y)$ and $b_n(x,y)$ would be independent of position if the illumination is uniform in each window at the input plane. Otherwise, $a_n(x,y)$ and $b_n(x,y)$ can be smooth functions of the position and, in such a case they must give rise to corresponding spectra of a given extension, however small.

In the practice, $n=0,1$ are two cases of interest, for $n=0$ the window of observation would be $w[x+x_0/2,y]$ and Eq. (8) could be reduced to

$$a_0(x,y)=\frac{1}{4}\cos^2\psi_0 I_A(x,y)+\frac{1}{\pi^2}\sin^2\psi_0 I_B(x,y), \tag{9a}$$

$$b_0(x,y)=\frac{1}{2\pi}\sin(2\psi_0)\sqrt{I_A(x,y)I_B(x,y)}, \tag{9b}$$

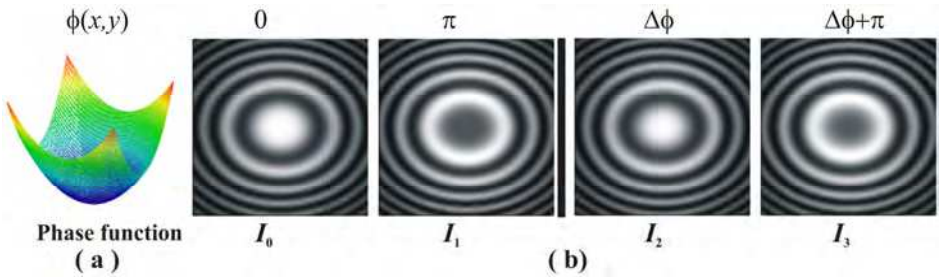

Fig. 2. Numerical simulation of phase shifting interferometry for four unequal phase-steps, which are obtained with two camera shots, that is with $N=2$, then $2N=4$ interferograms changed in phase are obtained: (a) phase function considered in this simulation and (b) for interferograms changed in phase by $\varphi=0,\Delta\phi,\pi,\Delta\phi+\pi$.

and for $n=1$ the window of observation would be $w[x-x_0/2,y]$ and Eq. (8) could be reduced to

$$a_1(x,y)=\frac{1}{\pi^2}\cos^2\psi_1 I_A(x,y)+\frac{1}{4}\sin^2\psi_1 I_B(x,y), \tag{10a}$$

$$b_1(x,y)=\frac{1}{2\pi}\sin(2\psi_1)\sqrt{I_A(x,y)I_B(x,y)}. \tag{10b}$$

Comparing Eq. (9) and Eq. (10) is easy to note that $a_0(x,y)$ and $a_1(x,y)$ in general are different and only they are equals in two cases:

case 1: when $I_A(x,y)=I_B(x,y)$, then from Eq. (9a) and Eq. (10a) must be complied

$$\frac{1}{4}\cos^2\psi_0+\frac{1}{\pi^2}\sin^2\psi_0=\frac{1}{\pi^2}\cos^2\psi_1+\frac{1}{4}\sin^2\psi_1, \tag{11}$$

which conduce to

$$\cos^2\psi_0+\cos^2\psi_1=1, \tag{12}$$

obtaining so

$$\cos\psi_0=\pm\sin\psi_1, \tag{13}$$

and finally can be established

$$\psi_0=\begin{cases}\pi/2-\psi_1\\ \pi/2+\psi_1\end{cases}, \tag{14}$$

which means that the polarizer placed at angle ψ_0 over the window $w[x+x_0/2,y]$ and the polarizer placed at angle ψ_1 over the window $w[x-x_0/2,y]$ could be at complementary angles, when $\psi_0=\pi/2-\psi_1$, or well could be at 90° each other, when $\psi_0=\pi/2+\psi_1$. For example: if $\psi_1=\pm45°$, then $\psi_0=45°$, or well $\psi_0=-45°$.

For the modulation light, in order to do $b_0(x,y)$ equal to $b_1(x,y)$ or $-b_1(x,y)$, from Eq. (9b) and Eq. (10b) it must be complied

$$\sin(2\psi_0)=\pm\sin(2\psi_1), \tag{15}$$

whereof can be deduced

$$\psi_0=\begin{cases}\pm\psi_1\\ \pm\pi/2\mp\psi_1\end{cases}, \tag{16}$$

a particular case of $\psi_0=\pm\psi_1$ in Eq. (16) would be only coincident with Eq. (14) for $\psi_1=\pm45°$ as it was written in the above example, but the case $\psi_0=\pi/2-\psi_1$ is totally coincident with Eqs. (14), so it can be used to apply to PSI technique.

case 2: when $I_A(x,y)\neq I_B(x,y)$, from Eq. (9a) and Eq. (10a) it must be complied

$$\frac{1}{4}\cos^2\psi_0 I_A(x,y)+\frac{1}{\pi^2}\sin^2\psi_0 I_B(x,y)=\frac{1}{\pi^2}\cos^2\psi_1 I_A(x,y)+\frac{1}{4}\sin^2\psi_1 I_B(x,y), \tag{17}$$

as a particular case, we can suppose

$$\frac{1}{4}\cos^2\psi_0=\frac{1}{\pi^2}\cos^2\psi_1 \text{ ; and } \frac{1}{\pi^2}\sin^2\psi_0=\frac{1}{4}\sin^2\psi_1, \tag{18}$$

whereof leads to plan a system of equations, where $\cos^2\psi_0$ and $\cos^2\psi_1$ would be the unknowns,

$$\begin{aligned} \pi^2\cos^2\psi_0 - 4\cos^2\psi_1 &= 0 \\ -4\cos^2\psi_0 + \pi^2\cos^2\psi_1 &= \pi^2 - 4 \end{aligned}', \tag{19}$$

being possible to found

$$\cos^2\psi_0 = \frac{4}{\pi^2+4}; \text{ and } \cos^2\psi_1 = \frac{\pi^2}{\pi^2+4}, \tag{20}$$

from Eq. (20) the following relation can be deduced

$$\cos^2\psi_0 = \sin^2\psi_1, \tag{21}$$

then, $\psi_0 = \pi/2 - \psi_1$, which are complementary angles, as in the *case 1* illustrated with Eq. (14). Finally, taking in account Eq. (20) the values of the polarizer angles can be computed,

$$\psi_0 = \pm 57.51°; \text{ and } \psi_1 = \pm 32.49°. \tag{22}$$

these values for transmission angles of the polarizers also must comply $b_0(x,y) = b_1(x,y)$ or $b_0(x,y) = -b_1(x,y)$ due to they are a particular case of Eq. (16).

In order to achieve the PSI technique, selecting P_3 at angle $\psi_0 = 45°$ for $n = 0$ and P_4 at angle $\psi_1 = -45°$ for $n = 1$ with no grating displacement, $u_0 = 0$, with idea to implemented *case 1* [Meneses-Fabian, et. al., 2009], this results $a_0(x,y) = a_1(x,y) = a(x,y)$ and also $b_0(x,y) = -b_1(x,y) = b(x,y)$, and of this manner two complementary patterns are first obtained at the image plane within replication regions given by $w[x + x_0/2, y]$ and $w[x - x_0/2, y]$. The possible changing in the fringe modulations was narrowly reduced after a normalization procedure, since the interferograms can be converted in digital patterns with the same modulation. Such patterns can be written as

$$I_0(x,y) = a(x,y) + b(x,y)\cos[\phi(x,y)], \tag{23a}$$

$$I_1(x,y) = a(x,y) - b(x,y)\cos[\phi(x,y)]. \tag{23b}$$

They correspond to patterns with a phase shift of $\alpha_1 = \pi$. Secondly, by performing an arbitrary translation of value $0 < u_0 < u_d/2$, the introduced phase shift is less than π radians. Then, another two interferograms result. Each one can be expressed as follows

$$I_2(x,y) = a(x,y) + b(x,y)\cos[\phi(x,y) - \Delta\phi], \tag{23c}$$

$$I_3(x,y) = a(x,y) - b(x,y)\cos[\phi(x,y) - \Delta\phi]. \tag{23d}$$

The corresponding phase shift for them is $\alpha_3 = \pi$. Considering patterns I_1 and I_2 they differ by a phase shift of $\alpha_2 = \Delta\phi - \pi$, where $\Delta\phi = 2\pi \cdot u_0 / u_d$. With this procedure, four

interferograms with phase displacements of $\varphi_0 = 0$, $\varphi_1 = \pi$, $\varphi_2 = \Delta\phi$, $\varphi_3 = \Delta\phi + \pi$ can be obtained using only an unknown grating shift and, thus, two camera shots. The desired phase distribution can be calculated from

$$\phi_w(x,y) = \arctan\left\{\frac{I_2(x,y) - I_3(x,y) - \left[I_0(x,y) - I_1(x,y)\right]\cos(\Delta\phi)}{\left[I_0(x,y) - I_1(x,y)\right]\sin(\Delta\phi)}\right\}, \tag{24}$$

where ϕ_w denotes the wrapped phase to be unwrapped further. From Eq. (24), for the case of $\Delta\phi = 90°$, the well-known formula for four shifts can be obtained (Schwider, 1990). Eq. (25) requires, of course, the knowledge of the value $\Delta\phi$ to be useful. In order to calculate $\Delta\phi$ from the same captured interferograms, the procedure suggested by (Kreis, 1986) can be applied. This procedure is based on the Fourier transform analysis of fringes and a variant of it is proposed in the following sections to conceal it with the desired phase extraction.

For the case 2, the polarizer angle must be placed to $\psi_0 = 57.51°$ and $\psi_1 = -32.49°$ in order to keep constant the visibility in the interference pattern as it was made in *case 1*, this manner the same structure of Eq. (23) could be obtained and the solution for the wrapped phase is obtained with the same Eq. (24). Note that the *case 2* is more general, so also the polarizer angle $\psi = \pm 57.51°$ is also valid for the case 1.

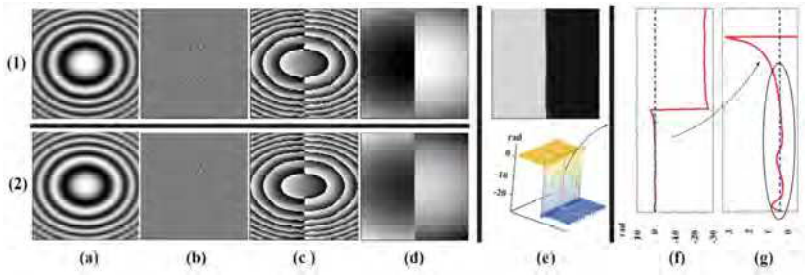

Fig. 3. Numerical simulations for determination of $\Delta\phi$ by using the modified Kreis method: (a) Patters indicated in Eq. (25), (b) Fourier transform from Eq. (25a) and spectrum filtered, (c) wrapped phases, (d) unwrapped phases, (e) phase difference of the unwrapped phases in (b1) and (b2), (f) a data line from (e), (g) subsample of the data line in (f).

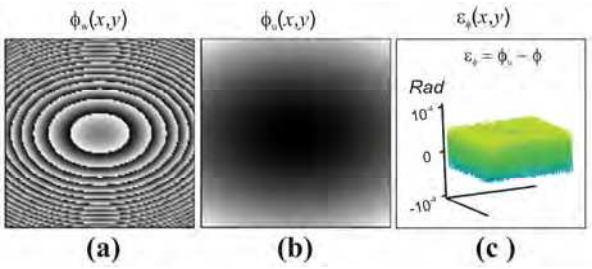

Fig. 4. Numerical simulations of phase extraction: (a) wrapped phase obtained with Eq. (24), (b) unwrapped phase, and (c) phase difference between the calculated phase in (b) and the proposal phase in Fig. (2.a) as a measurement of the error.

2.2 Determination of $\Delta\phi$

Subtraction of Eq. (23b) from Eq. (23a) and Eq. (23d) from Eq. (23c) gives

$$g_1(x,y) = I_0(x,y) - I_1(x,y) = 2b(x,y)\cos\left[\phi(x,y)\right], \tag{25a}$$

$$g_2(x,y) = I_2(x,y) - I_3(x,y) = 2b(x,y)\cos\left[\phi(x,y) - \Delta\phi\right], \tag{25b}$$

procedure which eliminates $a(x,y)$. In Eq. (25), some dependence on position has been considered to include effects such as non uniform illumination, non linear detection or imperfections in the optical components. These subtractions avoid to apply the Fourier transformation and the spatial filtering usually performed for the same purpose of eliminating $a(x,y)$ (Kreis, 1986). It is remarked that the Fourier transform procedure to eliminate $a(x,y)$ introduces an error due to the fact that, in general, the spectra from $a(x,y)$ and $b(x,y)\cos\phi(x,y)$ can be found mixed one with each other over the Fourier plane. Therefore, filtering out the $a(x,y)$ -spectrum around the zero frequency excludes also low frequencies from $b(x,y)\cos\phi(x,y)$ and, as a consequence, there is a corresponding loss of information related to $\phi(x,y)$ and $\Delta\phi$. To calculate $\Delta\phi$, the method introduced by (Kreis, 1986) is employed (an alternative can be seen in (Meng, et. al., 2008). An advantage of the variant that is proposed in this work consists of the elimination of $a(x,y)$ by subtracting two patterns. This way, there is no loss of information due to frequency suppression in the Fourier plane, as is the case of the method as proposed by (Kreis, 1990). The proposed technique is illustrated in the example of the Fig.2. In addition, the technique is valid even when the phase function is more complex. The 3-D plot at the left is the phase distribution $\phi(x,y)$, while the other plots are phase-shifted interferograms calculated from $\phi(x,y)$. Interferograms I_0 and I_1 are mutually shifted by π radians, as well as I_2 and I_3, but between I_0 and I_2, and I_1 and I_3 is the same arbitrary phase of $\Delta\phi = \pi/7 \approx 0.39269908$ radians. This situation illustrates the kind of results that can be obtained with the setup of Fig.1. Then, the problem is to find $\Delta\phi$ from the four interference patterns assuming that its value is not known. The solution is illustrated in Fig.3. The plots included are shown as an array of rows (seven letters) and columns (two numbers).

According to Eqs. (25.a) and (25.b), Figs.3-a1 and 3-a2 show the subtractions $g_1(x,y)$ and $g_2(x,y)$ respectively, where the four irradiances I_k were taken from the same interferograms of Fig. 2. Next, Fig. 3-b1 shows the Fourier spectrum of 3-a1 only ($g_1(x,y)$), while Fig. 3-b2 depicts its resulting filtered spectrum in accordance with the method of

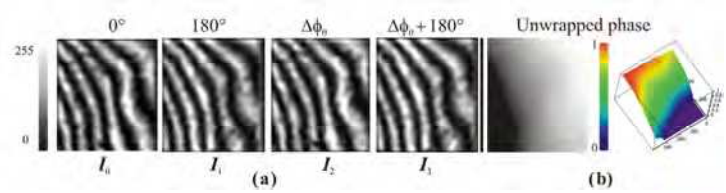

Fig. 5. Tilted wavefront for testing. (a) Interference patterns. (b) Unwrapped phase. Phase shift measured according to the modified Kreis method: $\Delta\phi = 14.4° = 0.2513274$ radians.

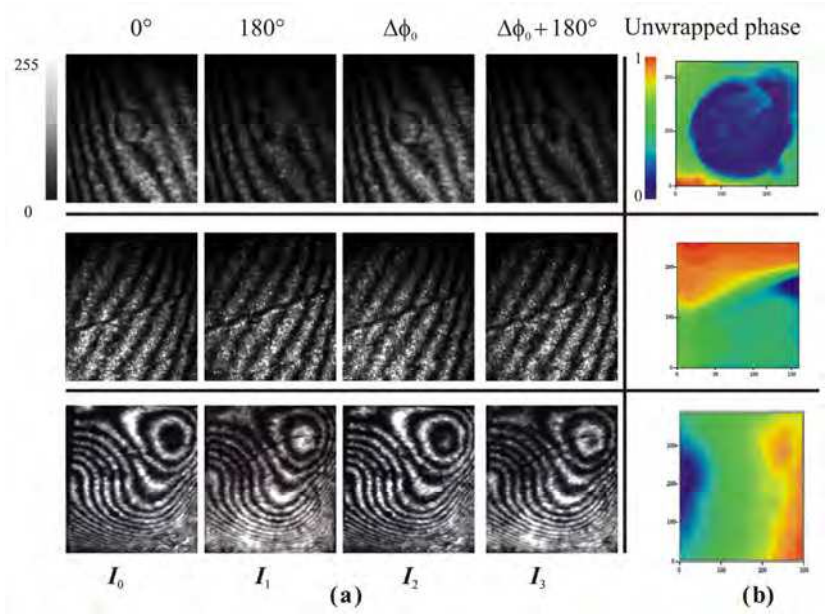

Fig. 6. Test objects. (a) Interference patterns (b) Unwrapped phase. Upper row: phase dot, $\Delta\phi = 50.007° = 0.874$ radians. Central row: phase step, $\Delta\phi = 25.726° = 0.449$ radians. Lower row: still oil, $\Delta\phi = 60.7° = 1.059$ radians.

Kreis. The used filter is a unit step, so the suppression of the left half of the spectrum is achieved. The following stage of the procedure to find $\Delta\phi$ consists of extracting the wrapped phase from the inverse Fourier transform of the already filtered $g_1(x,y)$, which is shown in Fig. 3-c1. Fig. 3-c2 shows the same procedure as applied to Fig. 3-2a (i.e., $g_2(x,y)$). At this stage, the phases of the inverse Fourier transform of each filtered interference pattern $g_1(x,y)$ and $g_2(x,y)$ are obtained. Therefore, these phases are wrapped, modified phases whose respective numerical integration results in two unwrapped, modified phases (Figs. 3-d1 and 3-d2). These unwrapped phases result in monotonous functions which are different from the desired phase ϕ, but their difference in each point (x,y) gives the modified phase difference $\Delta\phi'$ (Figs. 3-e). This modified phase difference has to be constant for all interference pattern points, so an average over some range can be sufficient to calculate $\Delta\phi$ with a good approximation. Fig. 3-f shows a line of Fig. 3-e1, and Fig. 3-g shows a section of the Fig. 3-f, where the used region to measure phase difference is indicated with an elliptic trace. The dots show the ideal phase difference $\Delta\phi$, while the red line shows the modified phase difference $\Delta\phi'$. The resulting value over the entire lower region of Fig. 3-e2 was of $\overline{\Delta\phi'} = 0.39273364$, where the bar means average, so its difference with respect to the initial induced phase $\Delta\phi$ is of the order of 3.4556×10^{-5} rads. Taken $\overline{\Delta\phi'}$ as $\Delta\phi$, the wrapped phase distribution ϕ_w can be determined with Eq. (24) and the desired phase distribution ϕ can be identified with ϕ_u, the phase calculated from ϕ_w with standard unwrapping algorithm [Malacara, et. al., 1998]. The results of these stages are shown in Fig. 4.

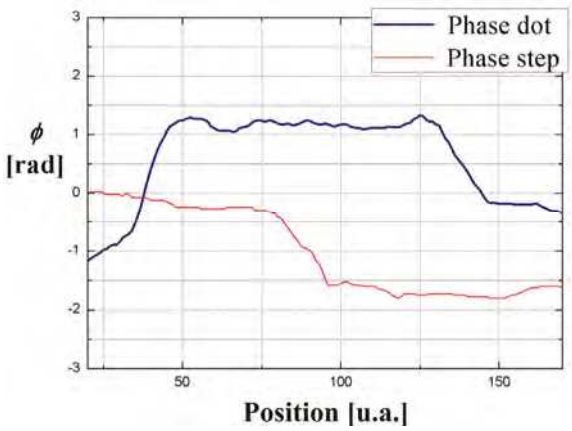

Fig. 7. Typical slice profiles of the phase dot and the phase step along arbitrary directions.

3. Experimental results

The experimental setup follows closely the sketch of Fig.1, with $f = 479mm$, a laser He-Ne emitting at $\lambda = 632.8nm$, with a linear polarization at 45° by using P_0. $a_w = 10mm$, $b_w = 13mm$, and $x_0 = 12.45mm$, so the condition $a_w < x_0$ is fulfilled. The period of the Ronchi grating was $u_d = 25.4\mu m$. The grating was mounted on an actuator (Newport CMA-25CC). Note that the diffraction-order matching condition $x_0 = N_0(\lambda f / u_d)$ for $N_0 = 1$ is satisfied. The CCD camera (COHU 4815) is adjusted to capture the images of two interference patterns ($w[x + x_0/2, y]$ and $w[x - x_0/2, y]$) simultaneously. The fringe modulations of this interferogram pair are mutually complementary. By one actuator displacement, another pair of complementary interferograms can be obtained. This is shown in Fig. 5, where the calculated value of the introduced phase was of $\Delta\phi = 14.4° = 0.2513274$ radians. The unwrapped phase is also shown. Each captured interferogram was subject to the same processing so as to get images with gray levels ranging from 0 to 255 before the use of Eq. (8). The sets of interferograms from three more objects are shown in Fig. 6. Two of these objects were prepared by evaporating magnesium fluoride (MgF2) on glass substrates (a phase dot, upper row, and a phase step, center row). The third object was oil deposited on a glass plate (bottom row). Each object was placed separately in one of the windows using the interferometer of Fig.1. Each set of four interferograms were obtained with a grating displacement between two of them as described. En each example, the phase-shifts induced by polarization can be visually identified from the complementary modulation contrasts of each pair. The calculated unwrapped phase for each object is shown in the rightmost column. Two typical profiles for some unwrapped phase are shown in Fig. (7). The resulting unwrapping phases do not display discontinuities, as is the case when the wrong $\Delta\phi$ is taken in Eq. (8).

4. Conclusion

The proposed phase-shifting interferometer is able to capture four useful interferograms with only one grating displacement and two shots. This grating displacement only requires

being smaller than a quarter of period, but this condition is possible to verify by observing that the fringes do not shift enough to adopt a complementary fringe modulation. Because in this proposed method the phase shifts are achieved either by modulation of polarization or by grating displacement, not all of the shifts result necessarily of the same value. The requirements of the arrangement are not very restrictive because it uses only very basic optical components, such as linear polarizers at angles of 0°, ±45°, or 90°. A Ronchi grating from 500 to 1500 lines per inch can be used. As remarked before, the higher the grating frequency, the larger the distance between windows and more space to place samples becomes available, but the grating displacement has to be smaller. This last feature does not represent an impediment in this method because the actuator responsible for the displacement does not need of a calibration within a certain range, neither a precise displacement at a given prescribed value. Only one unknown displacement is needed and its value can be calculated each time it is employed. As for the fringe modulation, it is close to unity when using the 0 and ±1 diffraction orders for a typical Ronchi grating. Also, the two used patterns have the same fringe modulation because, as long as the two diffraction orders which superpose are of equal value, the involved amplitudes are the same. These features to extract static phase distributions make this proposal competitive as compared to the existing ones. Although in this chapter was discussed the PSI method for four steps, this proposal can be extended for $N \geq 3$, with which $2N$ interferograms changed in phase would be obtained with N camera shots.

5. Acknowledgment

This work was partially supported from VIEP-BUAP under grant MEFC and PROMEP under grant PROMEP/103.5/09/4544) are greatly appreciated.

6. References

Arrizon, V. & De-La-Llave, D. (2004) Common-path interferometry with one-dimensional periodic filters, *Optics Letters*, Vol. 29, 141-143

Barrientos-García B.; Moore A. J.; Perez-Lopez C.; Wang L. & Tshudi T. (1999). Transient Deformation Measurement with Electronic Speckle Pattern Interferometry by Use of a Holographic Optical Element for Spatial Phase Stepping, *Applied Optics*. Vol. 38, 5944-5947, ISSN 1559-128X

Born, M. and Wolf, E.; Cambridge University Press (1993). *Principles of Optics*

Bruning, J. H.; Herriott, D. R.; Gallagher, J. E.; Rosenfeld, D. P.; White, A. D. & Brangaccio, D. J. (1974) Digital wavefront measurement interferometer for testing optical surfaces and lenses, *Applied Optics*, Vol. 13, pp. 2693-2703.

Creath K., "Phase-measurement interferometry techniques," Progress in Optics, Vol. XXVI, E. Wolf, ed., (Elsevier Science, 1993), pp. 349-393.

Hariharan, P.; Oreb, B. F.; Eiju, T. (1987) Digital phase-shifting interferometry: a simple error-compensating phase calculation algorithm, *Applied Optics*, Vol. 26, 2504-2506

Hech E.; Addison-Wesley (1972). *Optics*

Kreis, T. (1986). Digital holographic interference-phase measurement using the Fourier-transform method, *Journal of the Optical Society of America A*, Vol. 3, 847-855.

Kreis, T.; WILEY-VCH Verlag GmbH & Co. KGaA (2005). *Handbook of Holographic interferometry, optical and digital methods*

Malacara, D.; Servín, M.; & Malacara, Z.; Marcel Dekker, New York (1998). *Interferogram Analysis for Optical Testing*

Malacara D.; Wiley (2007). *Optical Shop Testing*

Meneses-Fabian, C.; Rodriguez-Zurita, G.; Vazquez-Castillo, J. F.; Robledo-Sanchez C. & Arrizon, V. (2006) Common-path phase-shifting interferometry with binary pattern, *Optics Communications*, Vol. 264, 13-17.

Meneses-Fabian, C.; Rodriguez-Zurita, G.; Encarnacion-Gutierrez, Ma. C. & Toto-Arellano N-I. (2009). Phase-shifting interferometry with four interferograms using linear polarization modulation and a Ronchi grating displaced by only a small unknown amount, *Optics Communications*, Vol. 282, 3063-3068.

Meng, X. F.; Cai, L. Z.; Wang, Y. R.; Yang, X. L.; Xu, X. F.; Dong, G. Y.; Shen, X. X. & Cheng, X. C. (2008). *Optics Communications*, Vol. 281 5701–5705.

Millerd J. E. & Brock N. J. (2003). Methods and apparatus for splitting, imaging, and measuring wavefronts in interferometry, U. S. Patent 20030053071A1.

Moore, A. J. & Mendoza-Santoyo, F., (1995). Phase demodulation in the space domain without a fringe carrier, *Optical Laser Engineering*, Vol. 23, pp. 319–330.

Nomura,T.; Murata, S.; Nitanai, E. & Numata, T. (2006). Phase-shifting digital holography with a phase difference between orthogonal polarizations, *Applied Optics*, Vol. 45 4873-4877.

Novák, M.; Millerd, J.; Brock, N.; North-Morris, M.; Hayes, J. & Wyant, J. (2005). Analysis of a micropolarizer array-based simultaneous phase-shifting interferometer, *Applied Optics*, vol. 44, pp. 6861-6868, ISSN 1559-128X.

Novák, J.; Novák, P. & Mikš, A. (2008) Multi-step phase-shifting algorithms insensitive to linear phase shift errors, *Optics Communications*, Vol. 281, 5302–5309

Peng, X.; Zhou, S. M. & Gao Z. (1995). An automatic demodulation technique for a non-linear carrier fringe pattern, *Optik*, Vol. 100, pp. 11–14.

Rodriguez-Zurita, G.; Meneses-Fabian, C.; Toto-Arellano, N. I.; Vazquez-Castillo, J. & Robledo-Sanchez C. (2008a), One-shot phase-shifting phase-grating interferometry with modulation of polarization: case of four interferograms, *Optics Express*, Vol. 16 9806-9817

Rodriguez-Zurita, G.; Toto-Arellano, N. I.; Meneses-Fabian, C. & Vazquez Castillo, J. (2008b) One-shot phase-shifting interferometry: five, seven, and nine interferograms, *Optics Letters*, Vol. 33, 2788-2790

Schreiber, H. & Bruning, J.H., (2007). Phase shifting interferometry, Chapter 14, in: *Optical Shop Testing*, D. Malacara Ed., Wiley & Sons, New York, 547-655.

Schwider, J. "Advanced Evaluation Techniques in Interferometry," Progress in Optics. Vol. XXVIII, E. Wolf, ed., (Elsevier Science, 1990), pp. 274-276.

Shamos, M. (1959). Great experiments in Physics, pp. 96-101, Holt Reinhart and Winston, New York

Takeda M., Ina H., and Kobayashi S., (1982). Fourier-Transform Method of Fringe-Pattern Analysis for Computer-Based Topography and Interferometry, *Journal of the Optical Society of America A*, Vol. 72, pp. 156-160

Xu, X. F.; Cai, L. Z.; Wang, Y. R.; Meng, X. F. & Sun, W. J. (2008). Simple direct extraction of unknown phase shift and wavefront reconstruction in generalized phase-shifting interferometry: algorithm and experiments, *Optics Letters*, Vol. 33, 776-778.

Young, T. (1804). Experimental demonstration of the general law of the interference of the light, *Philosophical transactions of the Royal Society of London*, Vol. 94, 2

Interferometry - Research and Applications in Science and Technology

Edited by Dr Ivan Padron

ISBN 978-953-51-0403-2
Hard cover, 462 pages
Publisher InTech
Published online 21, March, 2012
Published in print edition March, 2012

This book provides the most recent studies on interferometry and its applications in science and technology. It is an outline of theoretical and experimental aspects of interferometry and their applications. The book is divided in two sections. The first one is an overview of different interferometry techniques and their general applications, while the second section is devoted to more specific interferometry applications comprising from interferometry for magnetic fusion plasmas to interferometry in wireless networks. The book is an excellent reference of current interferometry applications in science and technology. It offers the opportunity to increase our knowledge about interferometry and encourage researchers in development of new applications.

InTech Europe
University Campus STeP Ri
Slavka Krautzeka 83/A
51000 Rijeka, Croatia
Phone: +385 (51) 770 447
Fax: +385 (51) 686 166
www.intechopen.com

InTech China
Unit 405, Office Block, Hotel Equatorial Shanghai
No.65, Yan An Road (West), Shanghai, 200040, China
中国上海市延安西路65号上海国际贵都大饭店办公楼405单元
Phone: +86-21-62489820
Fax: +86-21-62489821